ISSN 0747-9239, Seismic Instruments, 2021, Vol. 57, No. 4, pp. 384–396. © Allerton Press, Inc., 2021.
Russian Text © The Author(s), 2021, published in Seismicheskie Pribory, 2021, Vol. 57, No. 1, pp. 29–48.

Broadband Measuring Complex with Pseudonoise Signals for Electromagnetic Monitoring of Modern Geodynamic Processes in Seismically Active Zones

V. V. Bobrovsky[a], *, P. V. Ilyichev[a], and O. A. Lashin[a]

[a] *Research Station of the Russian Academy of Sciences, Bishkek, 720049 Kyrgyz Republic*

**e-mail: bvlad77@mail.ru*

Received December 22, 2020; revised March 10, 2021; accepted March 12, 2021

Abstract—The article presents a new electric exploration measuring complex with pseudonoise sounding signals. The complex is designed for sounding of the Earth's crust using transient electromagnetic methods. The technical characteristics of the complex and results of the first field experiments in the territory of the Bishkek geodynamic test area are presented. The tasks are set to improve the technical and operational characteristics of the complex, the implementation of which will allow the developed measuring complex to improve the technology for electromagnetic monitoring of the crust carried out at the Research Station of the Russian Academy of Sciences.

Keywords: geoelectrical exploration, electromagnetic monitoring of the crust, pseudonoise signals, correlation processing of signals, structural disturbances

DOI: 10.3103/S0747923921040034

INTRODUCTION

The main direction of research carried out at the Scientific Station of the Russian Academy of Sciences (SS RAS) is the study of geodynamic processes occurring in the depths of the earth's crust. The aim of the research is to predict hazardous (destructive) natural phenomena, such as earthquakes, causing vast destruction and loss of life. To solve these problems, in the territory of the Bishkek Geodynamic Testing Area (BGTA), which covers an area of about 25500 km^2, a system for electromagnetic monitoring of the stress-strain state of the crust was deployed (Groisman and Trapeznikov, 1986; Trapeznikov et al., 1997; Ilyichev et al., 2010), based on electric exploration sounding via field formation in the far zone (SFF) and providing monitoring of dynamic processes occurring in the crust at depths of up to 20 km.

The system consists of a powerful (180 kW) ERGU-600 electric exploration generator set (Volykhin et al., 1993; Trapeznikov and Turovsky, 1993), located in the center of BGTA (40 km south of Bishkek), and a network of receiving measurement points distributed over the test area. It is constantly being improved for new research problems and is currently being modernized to improve the technology for electromagnetic monitoring of the crust. One way to improve the system is to expand its capabilities by using, in addition to SFF, other passive and active electric exploration methods, in particular, magnetotelluric sounding (MTS) and the method of sounding by the formation of a field in the near zone (SNF).

This paper discusses the development of a new electric exploration measuring complex intended for sounding the crust with noise-like signals with a wide frequency spectrum. The construction of the measuring equipment is based on the well-known method of sensing by the formation of a field in the near zone (SNF). The difference between the new equipment and the existing SNF equipment lies in the use of special signals for sounding the crust in the form of noise-like continuously repeating sequences of bipolar rectangular pulses.

Noise-like signals (NLS) have long been successfully used in various fields of science and technology. The use of NLS in communication and information transmission systems (Varakin, 1985) and radar and radio navigation radically changed the technology of these systems and significantly increased the quality and reliability of information obtained. The idea of using NLS in electric exploration equipment occurred earlier. Despite this, to date, no working models of such equipment have been created. One of the first attempts to use NLS in active electric exploration is a study by Canadian specialists (Duncan et al., 1980).

Among other domestic advancements (ideas) on creating electric exploration equipment using NLS,

the invention by (Velikin, 2009) is noteworthy. The author proposed a new correlation method of pulsed electric exploration and a device for its implementation. A subsequent work (Velikin, A.B. and Velikin, A.A., 2016) describes the electric exploration method using special NLS and an experimental model of the STEM-1 software and hardware complex, designed for searching for and detecting minerals in the crust, in particular, hydrocarbons.

An advantage of the NLS method over the SFF method is that the offset between the source (induction probe frame) and observation point (signal sensor) can be significantly less than the investigated depth (Aleksanova et al., 2005). Due to the increased resolution of the NLS method, this method is used for more detailed study of the structure of the crust. It theoretically has no limitations on large sounding depths; however, in practice, such limitations exist, associated with signal recording in a very large dynamic range to reach large sounding depths. Estimated calculations show that for the range of sounding depths from 100 m to 10 km, taking into account the average resistivity of the equivalent homogeneous layer (204 Ω m), obtained from data of the average section of the electric structure of the crust in the BGTA, the dynamic range of the recorded signals should be at least 200 dB.

It is virtually impossible to obtain such a large dynamic range simply by improving the technical characteristics of the measuring equipment and using standard (known) algorithms for digital signal processing. To solve this problem in the developed measuring complex, special NLS pulse sequences with a large base ($B = \Delta f\tau > 100$) are used, where Δf is the width of the signal frequency spectrum; τ is its duration. In this case, during correlation processing of a received signal complicated by interference and uncorrelated noise, the probe signal provides much better noise and interference suppression of vs. classical sounding with deterministic signals.

The signal-to-noise ratio at the output of such a system increases by a factor of 100 or greater. In addition, correlation processing of the recorded signals makes it possible to directly obtain the pulsed transient response of the crust, since the pulsed transient response of the crust consists of the cross-correlation function between the recorded field formation signal and the probe signal (Ilyichev, 2012). By choosing the type of probing signals with a sufficiently large base, one can count on qualitative improvement in the measuring system vs. the existing systems. However, the power of the sounding generator set is significantly reduced.

In (Ilyichev and Bobrovsky, 2014), the authors presented the results of mathematical modeling of the measuring equipment, which confirmed the effective use of NLS in electric exploration equipment. In the time that has elapsed, a large amount of research and engineering works have been carried out at SS RAS to realize this idea, the features of NLS use have been revealed, and the requirements on the technical and operational parameters of the measuring equipment have been determined. As a result, an experimental prototype of the measuring complex with NLS (NLS EMC) was developed and manufactured. Below are the main results of the study.

ESTIMATION OF THE SIGNAL OF THE FIELD FORMATION LEVELS IN RELATION TO THE NLS METHOD FOR THE BGTA

When carrying out measurements by the NLS method using the electric exploration measuring complex NLSEMC, an installation with coaxial loops is used (Aleksanova et al., 2005). The source of the primary field is a square frame with an area $Q = 2500$ m^2.

The signal receiver in the NLS EMC is an integrating-type induction sensor that provides an output signal proportional to the magnetic field induction. After its correlation processing, the output signal will be proportional to the EMF induced in the sensor's measuring coil.

The equivalent area q of the measuring coil of this sensor, taking into account the field concentration in its core, is 800 m^2, which corresponds to a single-turn receiving frame 28 × 28 m in size. According to (Zhdanov, 1986), the EMF value in the receiving frame placed on the surface of a homogeneous half-space with resistivity ρ in the near zone of the induction source is determined by the expression

$$|\Delta U_{Bz}| = \frac{\mu_0 q Q I \left(\frac{\mu_0}{\rho}\right)^{3/2}}{10\pi^{3/2} t^{5/2}}, \quad (1)$$

where $\mu_0 = 4\pi \times 10^{-7}$ H/m is the magnetic constant; q is the area of the receiving frame (equivalent area of the sensor's measuring coil); Q is the area of the probe frame; I is the amplitude of current pulses in the probe frame; ρ is the electric resistivity of the medium (the crust); t is the current time, counted from the moment the current step is supplied to the probe frame.

The range of the measured (received) field formation signal for the monitored depths is determined as the ratio of the maximum and minimum EMF values in the sensor's receiving coil for the field formation times corresponding to the minimum and maximum sounding depths.

To determine the EMF according to (1), it is necessary to know the electric resistivity ρ of the medium and the field formation recording time t.

According to (Matveev, 1990), the field penetration depth (effective sounding depth) is determined by the recording time and electric resistivity of the medium:

$$z_{\text{eff}} \approx 0.71\sqrt{t\rho/\mu_r}, \quad (2)$$

Table 1. Average statistical section of electric structure of crust in BGTA

Layer no. i	Occurrence depth, m	Layer thickness h_i, m	Range of variations in electric resistivity of layer ρ_i, Ω m	Average statistical electric resistivity of layer ρ_i, Ω m
1	0–300	300	10–300	145
2	300–3000	2700	1000–3000	2000
3	3000–12000	9000	40–120	80
4	12000–25000	13000	1000–3000	2000

where ρ is the electric resistivity of the homogeneous half-space; t is the field formation recording time; μ_r is the relative magnetic permeability. In formula (2), z_{eff} is expressed in kilometers. For $\mu_r = 1$, it is possible to write

$$z_{\text{eff}} \approx 0.71\sqrt{t\rho}. \quad (3)$$

Then, the field formation recording time corresponding to a given effective sounding depth is determined as

$$t \approx \left(\frac{z_{\text{eff}}}{0.71\sqrt{\rho}}\right). \quad (4)$$

Let us consider a model of the probed medium (crust) in the form of a horizontally layered structure, each layer of which extends to infinity and has its own electric resistivity and thickness. Next, we determine the electric resistivity of an equivalent homogeneous layer corresponding to the given multilayer model. We obtain the average section of the electric structure of the crust for the BGTA. Table 1 shows the parameters of the average statistical section of the electric structure of the crust, obtained from data of earlier soundings of the crust by the frequency sounding (FS) and SFM methods at 22 points in the BGTA territory.

According to the equivalence rule, an expression can be written that relates the parameters of a multilayer horizontally layered medium with the parameters of an equivalent homogeneous layer (*Elektrorazvedka*, 1989):

$$\frac{h_{\text{e}}}{\rho_{\text{e}}} = \sum_{i=1}^{n}\frac{h_i}{\rho_i}, \quad (5)$$

where $h_{\text{e}} = \sum_{i=1}^{n} h_i = 25000$ m (see Table 1) is the thickness of the equivalent homogeneous layer; ρ_{e} is the electric resistivity of the equivalent homogeneous layer; ρ_i is the electric resistivity of the layer with the number i; h_i is the thickness of the layer with the number i; n is the number of layers under consideration.

The electric resistivity of the equivalent homogeneous layer according to (5) is determined as

$$\rho_{\text{e}} = \frac{h_{\text{e}}}{\sum_{i=1}^{n}\frac{h_i}{\rho_i}} = \frac{\sum_{i=1}^{n} h_i}{\sum_{i=1}^{n}\frac{h_i}{\rho_i}}. \quad (6)$$

Substituting the data in Table 1 into formula (6), let us calculate the average electric resistivity of the equivalent homogeneous layer of the crust for the BGTA:

$$\rho_{\text{es}} = \frac{25000}{\frac{300}{145}+\frac{2700}{2000}+\frac{9000}{80}+\frac{13000}{2000}} = 204\ \Omega\text{m}.$$

For sounding depths from 100 m to 10 km, using formula (4), we calculate the minimum ($t_{\min}$) and maximum ($t_{\max}$) field formation recording times for the obtained value ρ_{es}:

$$t_{\min} \approx \left(\frac{0.1}{0.71\sqrt{204}}\right)^2 = 9.72418\times10^{-5}\ \text{s};$$

$$t_{\max} \approx \left(\frac{10}{0.71\sqrt{204}}\right)^2 = 0.972418327\ \text{s}.$$

Substituting the obtained field formation recording times $t_{\min}$ and $t_{\max}$ and the electric resistivity ρ_{e} into formula (1), we calculate the maximum ($V_{\max}$) and minimum ($V_{\min}$) EMF induced in the sensor's measuring coil:

$$V_{\max} = \frac{\mu_0 qQI\left(\frac{\mu_0}{\rho_{\text{es}}}\right)^{3/2}}{10\pi^{3/2}t_{\min}^{5/2}} = 0.000234019\ \text{V},$$

$$V_{\min} = \frac{\mu_0 qQI\left(\frac{\mu_0}{\rho_{\text{es}}}\right)^{3/2}}{10\pi^{3/2}t_{\max}^{5/2}} = 2.34019\times10^{-14}\ \text{V}.$$

For the calculations, the following values were substituted: $Q = 2500$ m^2; $q = 800$ m^2; $I = 2$ A.

Based on this, we find the range of variation in the measured signals in the given depth range:

$$D = 20\log\frac{0.000234019}{2.34019\times10^{-14}} = 200\ \text{dB}.$$

All of the above calculations are valid only in the case when the near zone condition is fulfilled over the entire considered depth range. According to (Matveev, 1990), the near field condition can be represented as

$$\frac{r}{z_{\text{eff}}} < 1, \quad (7)$$

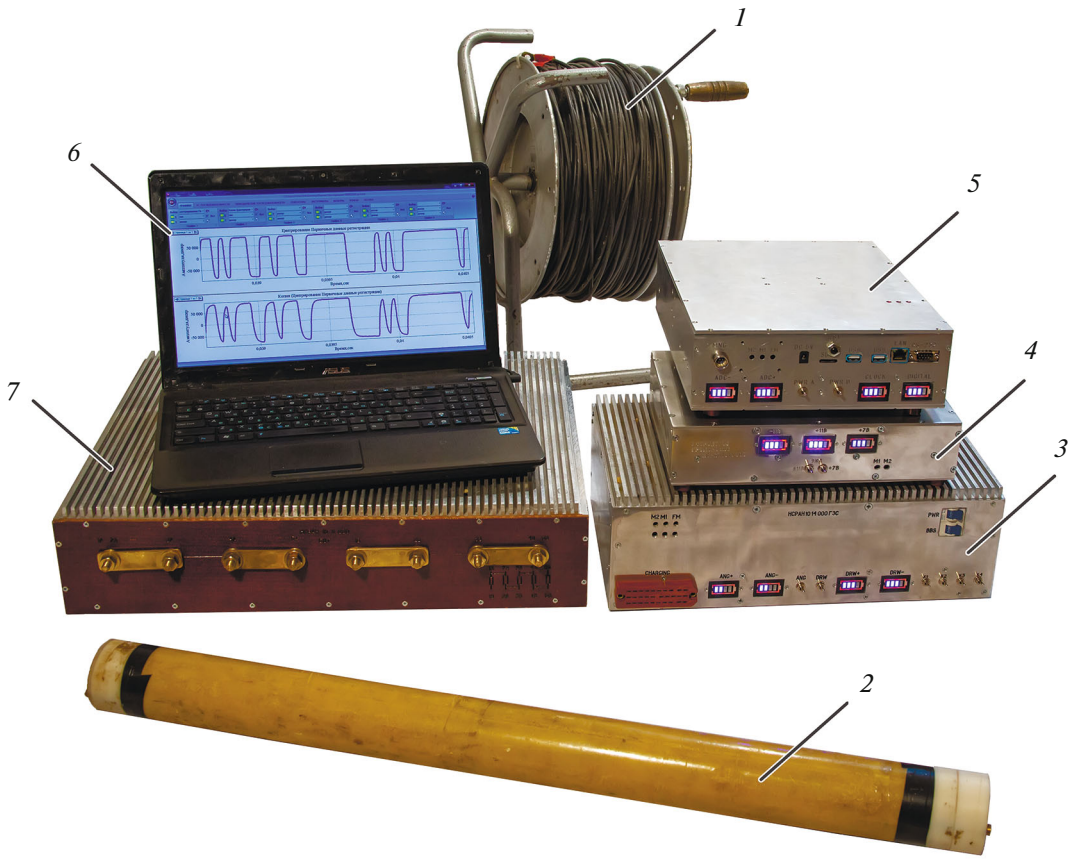

Fig. 1. Experimental prototype of NLS EMC measuring complex, external view: *1*, induction probing frame (IPF); *2*, induction signal sensor (ISS); *3*, probing signal generator (PSG); *4*, calibration unit (CU); *5*, signal control and recording unit (SCRU); *6*, laptop (PC); *7*, current limiting unit (CLU).

where z_{eff} is the effective sounding depth; r is the offset (distance between source and receiver). For a coaxial installation, the offset is equal to half the length of the side of the generator loop. For the square probe frame with a side of 50 m used in the NLS EMC, the r value will be 25 m. Substituting the offset value and the minimum considered depth into formula (7), the near field condition can be written as

$$\frac{r}{z_{\text{eff}}} = \frac{0.025}{0.1} = 0.25 < 1$$

(the r and z_{eff} values are given in km). Hence, it can be stated that the near zone condition is fulfilled over the entire considered depth range.

MEASURING COMPLEX HARDWARE

Figure 1 shows an external view of an experimental prototype of the NLS EMC.

The main task in developing a new measuring complex was to achieve the necessary dynamic and frequency ranges of recorded signals, which determine the monitored depths of the crust.

In developing the measuring equipment, modern multibit high-speed analog-to-digital converters (ADC) were used, which allow signal recording in wide dynamic and frequency ranges. The digital nodes and units of the measuring complex are made using modern FPGA technology, which significantly reduced the time to develop and debug the measuring equipment. To power the nodes and units of the new equipment, lithium-ion batteries were used, directly built into the structure of the equipment units, which ensured fairly low weight and small dimensions.

Figure 2 shows the structural–functional circuit of the measuring complex.

The measuring complex consists of two parts: probing and receiving–recording. The probing part includes a probe signal generator (PSG), an induction probe frame (IPF), a current limiting unit (CLU), and a rechargable battery (RB). The receiving and recording part includes an induction signal sensor (ISS), a signal control and recording unit (SCRU), and a calibration unit (CU).

The technical parameters of the measuring complex are given in Table 2.

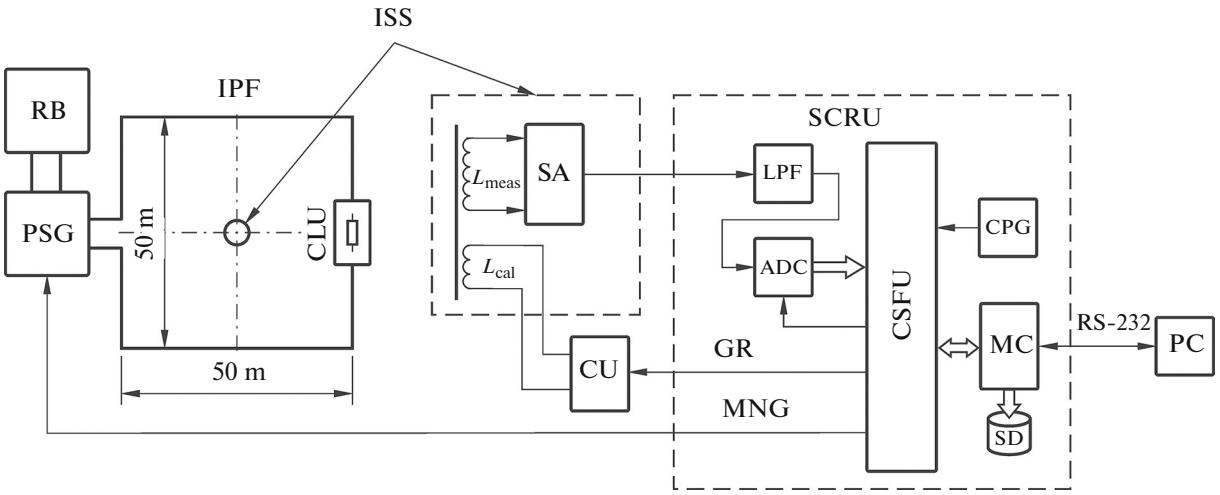

Fig. 2. Electric exploration measuring complex with NLS, structural and functional diagram: IPF, induction probing frame; CLU, current limiting unit; PSG, probe signal generator; RB, rechargable battery; ISS, induction signal sensor; SA, signal amplifier; CU, calibration device; SCRU, signal control and recording unit; ADC, analog-to-digital converter; CPG, clock pulse generator; LPF, low-pass filter; CSFU, control-signal-forming unit; MC, microcontroller; SD, memory card; PC, laptop; L_{meas} ISS measuring coil; L_{cal}, ISS calibration coil; GR, signals controlling CU operation; MNG, signals controlling PSG operation; RS-232, serial interface.

Table 2. Technical parameters of NLS EMC

Parameter	Measurement unit	Value	Note:
1	2	3	4
Receiving and measuring channel			
Bandwidth	Hz	0.4232000	
ISS conversion factor	mV/nT	75 ± 5	
ISS time constant	s	0.65	
Dynamic range of recorded signals, no less than	dB	180	
ADC bit capacity	bit	18–24	
Signal sampling rate	kHz	10.0–1638.4	
Duration of a single noiselike M-sequence	s	0.01–5.12	
Bit capacity of M-sequence	bit	11–24	
Probing unit			
IPF dimensions	m	50 × 50...200 × 200	
Inductance of IPF	mH	0.4–1.6	
Active resistivity of IPF	W	2–8	
Voltage of recharagable battery U_{RB}	V	12–250	
Active resistivity of CLU R_{CLU}	Ω	25–200	
Current pulse amplitude in IPF	A	1.0–10.0	Depends on R_{CLU} and U_{RB}
Minimum duration of current pulses in probe frame	μs	20	
Duration of current pulse rise and fall in probe frame	μs	12	For R_{CLU} = 100 Ω

The main unit of the measuring complex is the signal control and recording unit (SCRU). Functions performed by the SCRU:

— formation of logical signals and commands that ensure tuning of modes and synchronization of the operation of probing and receiving-recording parts of measuring complex;

— digitization of recorded signals;

— storage, accumulation, and computer transfer of digital data obtained in measurement sessions.

The operation of all digital SCRU circuits is clocked (synchronized) by a clock pulse generator (CPG) GK75-TS of the Morion company (St. Petersburg).

The microcontroller (MC), operating under the control of the BBS_Registrator_ADD recording program, generates commands that determine the SCRU operation modes, and records and stores the received data in an SD memory card. An SK-MAT91SAM9G45/M10 board (module) from STARTERKIT.RU (Izhevsk) is is used as the MC. Program–user interaction is through an external laptop computer (LC) using the program BBS_Terminal_ADD, working with an RS-232 serial input–output interface.

The control-signal-forming unit (CSFU), implemented on a DE0-Nano module from Terasic, based on a Cyclone IV EP4CE22F17C6N FPGA, provides connection and synchronous operation of all SCRU nodes (Lashin, 2018). MNG and GR signals are generated in the CSFU, which controls the operation of the PSG and CU.

When sounding the crust, the sequence of MNG signals generated in the CSFU arrives at the PSG (Lashin, 2019a), where, under their control, noiselike current pulse sequences are generated, which are fed through the current limiting unit (CLU) to the induction probe frame (IPF). To reduce the influence of interference generated by the transmission lines of digital control signals between the SCRU and the PSG, the length of which is about 40 meters, these circuits are made in the form of fiber-optic communication lines (Lisimov, 2019). The sounding frame is placed horizontally on the surface of the Earth. An induction signal sensor (ISS) is installed at vertically the geometric center of the frame.

The measuring complex uses a proprietary broadband temperature-compensated induction sensor (Ilyichev and Lashin, 2017). Alternating current induced in the short-circuited sensor's measuring coil (L_{meas}) and proportional to the magnetic flux penetrating the windings of this coil, with the help of an amplifier (AMP) is converted into voltage and amplified to the value necessary for conversion into digital form. The amplifier is placed in the immediate vicinity of the measuring coil inside the rigid housing of the sensor, whihc is made of an aluminum alloy and acts as an electric shield against external pickup and interference. The conversion factor of the ISS remains virtually unchanged in a broad frequency band (0.4–32000 Hz).

The output signal of the induction sensor, once it has passed through a low-pass filter (LPF) in the SCRU, is converted by an ADC into digital form. The ADC was a DC1826A module from Linear Technology, made on an LTC2389 microcircuit, which is a modern ADC manufactured by SAR technology with an 18-bit capacity and a maximum sampling rate of 2.5 MHz. The resulting digital data are recorded and stored in a MicroSD Card in the FAT file system. Then, the data are processed in a personal computer using the BBS_ViewerM_NR program developed by the authors.

To measure and monitor the technical characteristics and parameters of the measuring complex used when processing of sounding data, the measuring channel is provided with a calibration mode of. In this mode, under the control of GR signals generated by the SCRU, current pulses are formed in the CU, which are fed into the calibrating coil of the induction sensor (L_{cal}), which creates a calibrated alternating magnetic field in the measuring coil. The output signal of the analog part of the measuring channel (LPF output), just like in the case of a sounding session, is converted by the ADC into digital samples stored on an SD card. The recorded data are processed in a computer to obtain the transient, pulsed transient, and frequency characteristics of the measuring channel.

Another purpose of calibration is to guarantee the performance of the measuring complex. In the process of such a check, model signals of the formation of the field, formed in the CU and simulating a one-dimensional multilayer electric section of the crust, are fed into the calibration coil of the induction sensor. The calibration of the measuring channel of the EMC NLS is carried out before each measuring session.

When developing the circuit and design of the measuring complex, special attention was paid to the suppression of interference and noise, limiting the dynamic range of the recorded signals. To determine the requirements on the frequency response of the measuring channel, the spectral composition of interference and noise observed on the territory of the BGTA were measured at various points on the Earth's surface. The noise level was estimated in the frequency band from 20 Hz to 2 MHz. Interference was quantitatively assessed with a portable spectrum analyzer developed by one of the authors (Lashin, 2019b).

Measurements showed that the main sources of interference are an industrial power network with a frequency of 50 Hz and powerful radio stations operating in Kyrgyzstan. The level of interference from the industrial network did not exceed 5% of the maximum of the field formation signal recorded during sounding sessions of the crust with a 50 × 50 m induction frame

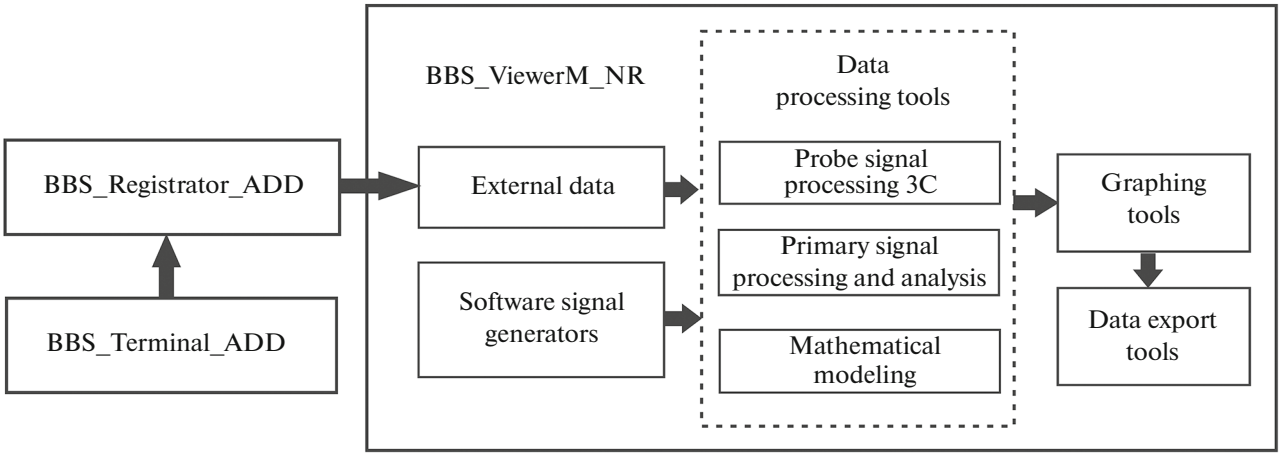

Fig. 3. Block diagram of NLS EMC software.

with rectangular current pulses with an amplitude of 1 A. The level of interference from radio stations localized in a narrow frequency band (5 kHz) with a center frequency of 612 kHz did not exceed 0.5% of the maximum level of the field formation signal.

Suppression of interference created by the industrial power network with a frequency of 50 Hz in the measuring complex is ensured by correlation processing of recorded signals and their synchronous accumulation in the time window. For this, the duration of the accumulation window is chosen as a multiple of an odd number of half-periods of the suppressed interference (10 ms) and is determined by the duration of three or five probing single noiselike M-sequences. In this case, the duration of a single M-sequence determines the maximum field formation time required to obtain the specified sounding depths. Sounding of the crust is carried out by continuously repeated pauseless bipolar M-sequences of rectangular current pulses supplied to the IPF for a time corresponding to the specified number of signal accumulation windows.

The LPF limits the spectrum of signals entering the ADC input and suppresses high-frequency interference from radio stations. The selected cutoff frequency (40 kHz) and the slope of the transition zone of the amplitude–frequency response (AFR) of this filter provide high interference suppression at frequencies above 600 kHz (by more than 30000 times, 90 dB). At the same time, reliable recording of field formation signals is ensured at times starting from 25 μs, which corresponds to sounding depths of 70 m or more. The strict monotonicity of the LPF's transient response ensures undistorted passage of field formation signals through the measuring channel. The filter circuit is an active eight-order low pass ladder filter with critical attenuation (Titze et al., 2007).

To assess the degree of influence of interference and noise on the quality of the recorded signals, an operational monitoring of the interference environment is carried out before each measurement session. The hardware and software of the measuring complex makes it possible to carry out such measurements with the required accuracy and to obtain an estimate of the spectral composition of interference and noise recorded by its measuring path.

Measuring Complex Software

The software package of the measuring complex consists of two parts: registering (programs BBS_Registrator_ADD and BBS_Terminal_ADD) and processing (program BBS_ViewerM_NR). In Fig. 3 shows the structure of the EMC NLS software.

The BBS_Registrator_ADD program, implemented in the C programming language, is designed to control the SCRU operation modes and provides recording and storage of data (signal samples) coming from the ADC output of the EMC ShPS measuring channel (Bobrovsky, 2020).

The control of the SCRU operation modes consists in processing the commands of the user (operator) setting the types and parameters of the control signals generated by the SCRU (MNG and GR, see Fig. 2), and converting them into the format necessary for the operation of the programmable control signal generation unit (CFCS, see Fig. 2). Under the control of the MNG and GR, probing and calibration signals are generated in the PSG and CU of the measuring complex in the form of sequences of current pulses supplied, depending on the operating mode, to the IPF or to the ISS calibration coil. Two types of sequences are used: noise-like bipolar pulse M-sequences, used both in the Crust sounding mode and in the calibration mode, and periodic sequences of bipolar pulses without a pause with the same duration of positive and negative pulses, used only in the calibration mode of the measuring channel.

Recording and storage of data coming from the ADC occurs during the interrupt processing on the readiness signal generated by the ADC. At the first stage, data is read from the ADC through the parallel input-output interface PIO (Parallel Input/Output Controller) built into the microcontroller (MC). Next, the data is converted into a signed integer format and written to the buffer memory, which is implemented as a circular buffer. To reduce the level of interference and noise in the recorded signals, the program implements an algorithm for synchronous accumulation of signal samples from the ADC in real time (on-line) with subsequent storage of the accumulated data on an external medium. The operation of the online accumulation algorithm is based on a circular buffer with a volume corresponding to a given accumulation window.

After filling the circular buffer, the incoming new signal samples are summed with the old ones. The width of the cells of the circular buffer is determined by the width of the ADC and the number of accumulated signal samples. Normalization of the recorded signal, which consists in dividing each sample of the circular buffer by the number of accumulations, is performed in the BBS_ViewerM_NR signal processing program. The use of the real time synchronous accumulation algorithm can significantly reduce the amount of data received while maintaining the duration of recording and number of accumulations, which increases the efficiency of processing and analysis of recorded data in the field with minimum computer system requirements.

For convenience of field operation with the recording program , the BBS_Terminal_ADD program was developed, designed to automate the process of controlling the signal recording modes and parameters. Standard (typical) terminal programs require the user to sequentially enter all recording parameters before each measurement session, whereas in the field, to obtain the necessary measurement statistics, it is often necessary to conduct a series of sessions with the same recording parameters or to conduct the same recording sessions at different measurement points.

To increase the speed of an operator's work, the program can change one or more recording parameters during operation and automatically transmit them to the recording program. Up to ten sets of recording parameters can be saved in a special configuration file, which can be quickly edited and uploaded.

The BBS_ViewerM_NR program is written in the Delphi programming environment and is designed to process data from model, laboratory, and field experiments on an external laptop (Bobrovsky and Ilyichev, 2018a). The processed data can be both external data obtained during recording from the NLS EMC measuring channel output and data generated by software (software signal generators). Data processing tools implemented in the program are conditionally divided into several groups.

The group "Processing of PS data" is a set of tools designed to process the recorded data from a field experiment in order to obtain the field formation curve and calculate the apparent resistivity of rocks at the point of the experiment.

The group "Primary signal processing and analysis" is a set of tools designed for primary signal processing and analysis. In addition to standard operations with signals (mathematical and arithmetical operations, digital filtering and spectral analysis tools, etc.), this group includes special tools designed for signal processing, taking into account the specific features of correlation processing of NLS. The output signals of the measuring channel of the NLS EMC recorded during the calibration process are processed with the tools of this group to obtain the transient, pulse, and frequency responses of the measuring channel.

The group "Mathematical Modeling" is intended to study the features of using NLS in active crustal electric exploration systems vs. typical systems with deterministic bipolar current pulse sequences of constant duration for sounding. The program implements mathematical models of electric exploration systems with noiselike and deterministic sequences of sounding pulses.

The model experiment makes it possible to obtain comparative data for two types of electric exploration systems, to quantify the gain in the signal-to-noise ratio obtained with NLS, and to optimally select the parameters of the system with NLS. The algorithms of the mathematical models and research results obtained using the tools of this group are described in more detail in (Ilyichev and Bobrovsky, 2014, 2018; Bobrovsky and Ilyichev, 2018b).

The group "Tools for working with graphs" is designed to display the results of the program in two- and three-dimensional graphs. The program allows simultaneously display of up to six graphs, for each of which individual settings of display parameters are available (scale settings, selection of line and text display parameters, etc.).

The group "Data export tools" makes it possible to save the results of the program in basic graphics (jpg, bmp, emf, wmf) or text (ASCII, XLS, XML, etc.) formats.

The BBS_ViewerM_NR program is described in more detail in (Bobrovsky and Ilyichev, 2019).

FIELD TESTS OF THE MEASURING COMPLEX

Field tests of the experimental sample of the measuring complex have commenced. Works were carried out at point MHD on the territory of SS RAS.

Table 3. Calibration pulse parameters

Calibration mode	Parameters		
	amplitude	duration, s	number of accumulations
SCRU calibration	±1.65 V	0.075	100
Measuring channel calibration (high frequencies)	±3.2 mA	0.1	100
Measuring channel calibration (low frequencies)		11.275	10

The SCRU was calibrated separately without the induction sensor and the measuring channel as a whole. The purpose of these calibrations is to obtain the pulsed transient and frequency responses of the SCRU and measuring channel in the field, compare them with the calculated ones, and check the performance characteristics of the measuring complex, including lower- and upper-level software operation. Table 3 gives the parameters of rectangular pulses applied to the SCRU input and to calibrating coil of the induction sensor.

Figure 4 shows the graphs of the transient (TR), pulsed transient (PTR) and amplitude–frequency (AFR) responses of the SCRU.

According to Fig. 4, the SCRU cutoff frequency obtained from the calibration results and determined at a level of –3 dB was $f_C = 40$ kHz; suppression of signals at frequencies of $2f_C = 80$ kHz and $4f_C = 160$ kHz were 11 and 31 dB, respectively, which fully corresponds to the calculated values.

Figure 5 shows the PTR and AFR of the measuring channel. According to Fig. 5, the cutoff frequency of the measuring channel in the low-frequency region determined at a level of –3 dB was 0.42 Hz; in the high-frequency region, 32 kHz. In the passband in the frequency range from 90 to 1000 Hz, there is an insignificant (about 1 dB) drop in the AFR, determined by the frequency response of the ISS.

Then, sounding of the crust was carried out with NLS. The aim of the experiment is to obtain the field formation curve (EMF induced in the sensor's measuring coil) and the apparent resistivity of rocks. Table 4 shows the parameters of the probing signals.

The field formation curve $e(t)$ was the accumulated correlation function (ACF) obtained in correlation signal processing, since in the time interval from $T_{min} = 41$ μs to $L_{MP} = 1.35$ s, the ACF values are proportional to the EMF values induced in the sensor's measuring coil (Ilyichev, 2012).

Figure 6 shows the graphs of the function $e(t)$ obtained after signal correlation processing (a) and

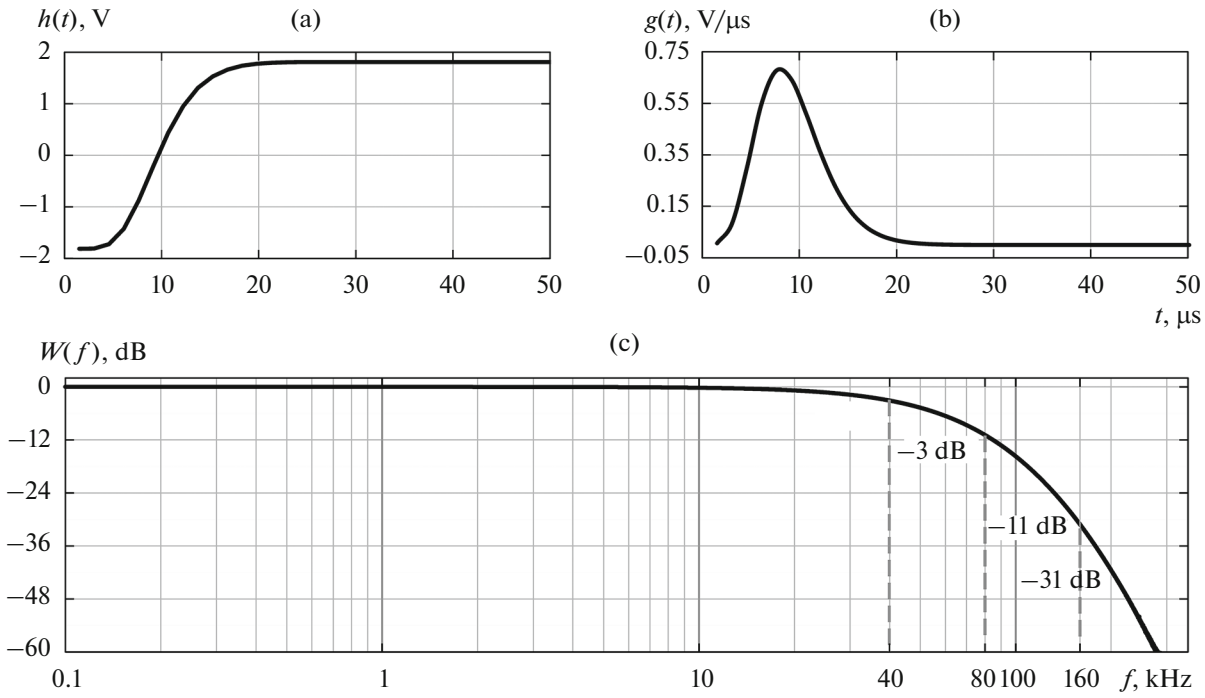

Fig. 4. SCRU calibration results: (a) TR, (b) PTR, (c) AFR.

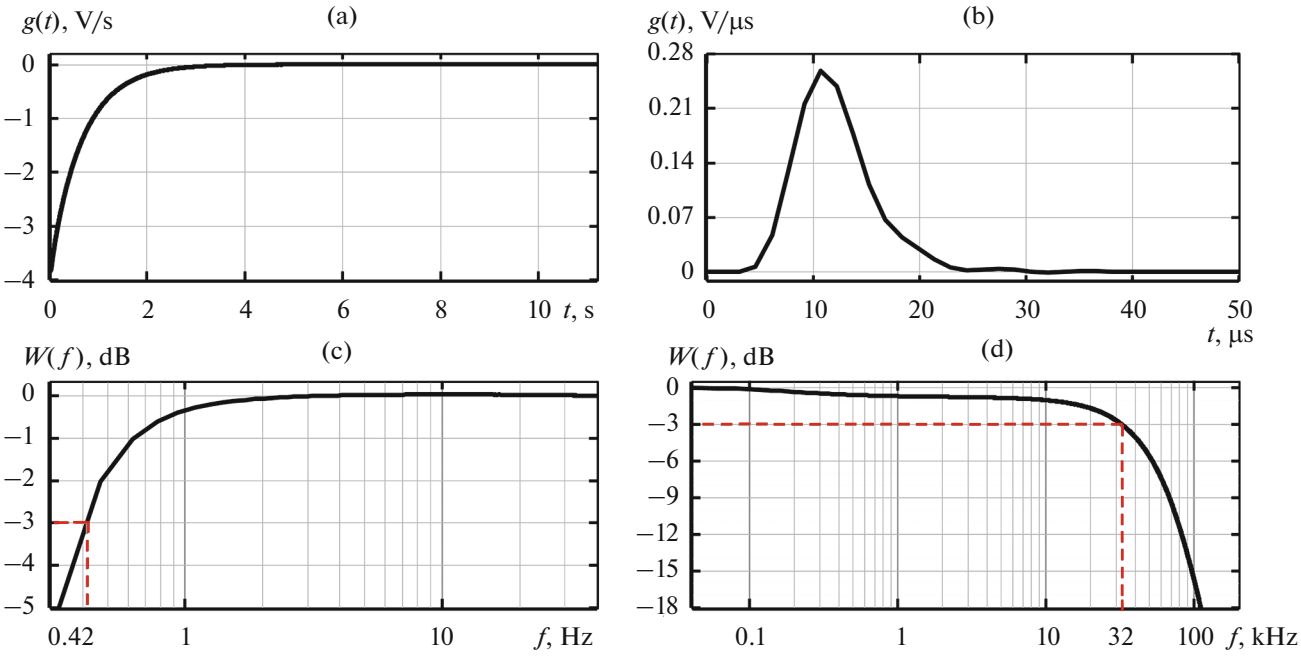

Fig. 5. Results of calibrating measuring channel of NLS EMC. (a) PTR in range of large times; (b) PTR in range of small times; (c) AFR in low-frequency range; (d) AFR in high-frequency region.

after removal of so-called structural interference (b). In order to reveal the shape of the field formation signal at long times, the graphs are shown on a scale stretched along the amplitude axis.

According to Fig. 6a, against a background of slow change $e(t)$, there are characteristic pulsed signals, structural interferences, that occur after correlation signal processing. The main reason for this interference is even very small (less than 0.01%) nonlinearities of the transfer characteristics of the elements making up the measuring system, including the probing part of the measuring complex, the object of study (crust), and the receiving part (measuring channel) (Bobrovsky and Ilyichev, 2018b). Since structural interference significantly limits the dynamic range of the recorded signals, a special algorithm and software for processing field formation signals were developed, which ensure the removal of such interference and do not distort the field formation signal itself (Fig. 6b).

In the range of long times, starting from 20 ms or more, the received signal $e(t)$ is complicated not only by structural interference, but also by interference remaining after correlation processing and accumulation. To suppress the remaining interference a digital LPF is applied using a third-order moving median Dirichlet filter with a rectangular window. As a result, in the signal $e(t)$ in the range of long times, all interference was almost completely eliminated. The dynamic range of the field formation signals recorded by the measuring complex was estimated according to the formula

$$D = 20\log\left(\frac{e_{\max}}{3\sigma}\right) = 180 \text{ dB},$$

where $e_{\max}$ is the initial signal value $e(t)$ at $t = T_{\min}$ (see Table 4); σ is the rms noise remaining after correlation processing and removal of structural noise.

Figure 7 shows on a logarithmic scale along the time and amplitude axes the entire field formation curve $e(t)$ after removal of structural interference.

Further processing of the field formation curve involved recalculation of the function $e(t)$ into the the apparent resistivity of rocks $\rho(t)$ according to a simplified formula valid for the near field (Aleksanova et al., 2005):

$$\rho(t) = \frac{\mu_0}{\pi t}\left(\frac{Qq\mu_0 I}{20te(t)}\right)^{2/3},$$

where $Q = 2500$ m^2 is the area of the probe frame; $q = 10\,925\,229$ m^2 is the equivalent area of the ISS measuring coil taking into account the magnetic core and transmission coefficient of the measuring channel; t is time; $e(t)$ is the EMF induced in the receiving frame;

Table 4. Probing signal parameters

I_Z, A	N_{MP}, bit	$T_{\min}$, μs	L_{MP}, s
±2.0	15	41	1.35

I_Z is the strength of the current pulses in the probe frame; N_{MS} is the bit capacity of the M-sequence; $T_{\min}$ is the minimum duration of pulses in the M-sequence; L_{MP} is the duration of the M-sequence.

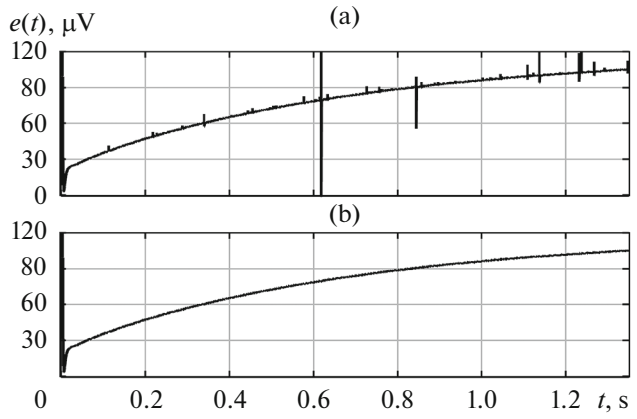

Fig. 6. Field formation curve: (a) obtained as a result of correlation processing of recorded signals; (b) after additional processing (removal of structural interference).

$\mu_0 = 4\pi \times 10^{-7}$ H/m is the magnetic constant; $I = 2.0$ A is the current pulse amplitude in the probe frame.

Figure 8 shows a graph of the apparent resistivity of rocks $\rho(t)$ plotted according to $e(t)$.

DISCUSSION

Analysis of the experimental data obtained with the new measuring complex (see Figs. 7, 8) shows that the field formation curve $e(t)$ and the apparent resistivity of rocks $\rho(t)$ in the time range from 2 to 20 ms are distorted. These distortions, according to (Svetov, 2008), may be the response from transient processes in the field of a vertical magnetic dipole. Thus, it can be stated that the measuring complex ensures control of the field formation curve due to the broad frequency range and large dynamic range of the recorded signals.

There is no doubt as to the need to further improve the measuring complex in order to expand its dynamic and frequency ranges, especially in the low-frequency region. To expand the frequency range in the low-frequency range, it is necessary to introduce another, lower-frequency, inductive signal sensor into the measuring complex. In this case, measurements will be carried out in two stages: for large field formation times (low frequencies) and short times (higher frequencies). It may be necessary to increase the duration of the probing M-sequences to 4–5 s with a simultaneous increase in their bit capacity. To increase the dynamic range of the recorded signals, it is necessary to increase the bit capacity of the ADC to 24 and the amplitude of the probing current pulses to 20 A. It may also be necessary to increase the dimensions of the probing frame to 100 × 100 m.

In the future, to obtain a geoelectric section, it is proposed to use one of the well-known methods for interpreting NLS data: the Sidorov–Tikshaev transform (Sidorov, 1985), solution of the inverse problem in any class of models (e.g., by the fitting method) or the method for determining the generalized parameters of the section from asymptotes and singular points (Aleksanova et al., 2005). All these problems are quite solvable.

In general, the completed development and first tests of the experimental prototype of the measuring complex show that, with the above modifications, the improved measuring complex can become a good addition to measuring equipment used as part of the

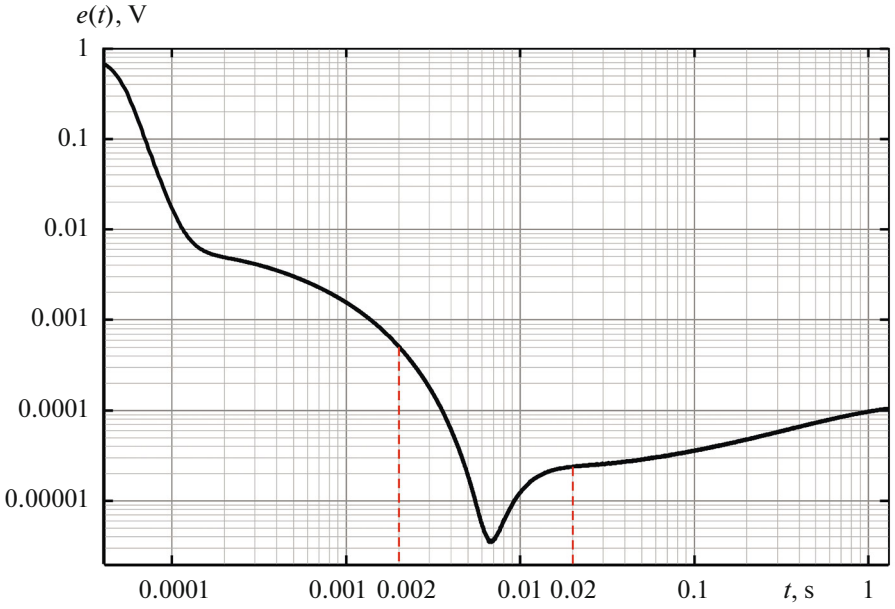

Fig. 7. Field formation curve obtained from data of field recording of received signals during sounding of crust.

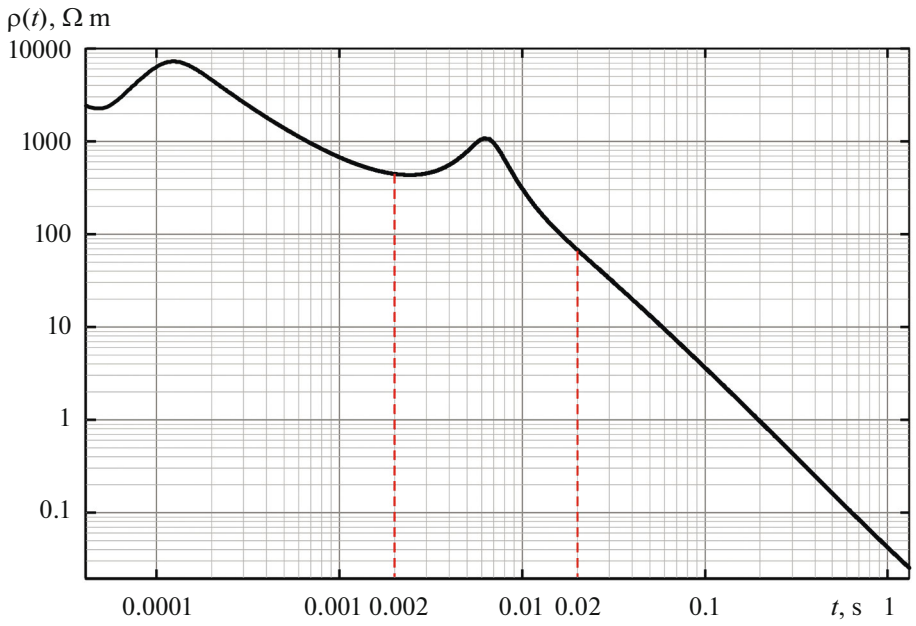

Fig. 8. Apparent resistivity of rocks.

electromagnetic crustal monitoring system operating in the BGTA.

ACKNOWLEDGMENTS

The authors express their deep gratitude to Anatoly Kuzmich Rybin, Doctor of Physics and Mathematics, and Pavel Nikolayevich Aleksandrov, Doctor of Physics and Mathematics, for advice and assistance in the writing of this article, as well as to the staff of the Laboratory of Advanced Hardware Development of RS RAS Maxim Olegovich Lisimov, Andrey Anatolyevich Pecherov, and Denis Vitalievich Kolomeytsev for active participation in the work and practical contributions to development of the topic.

FUNDING

The study was carried out within a state task on the topic: "Development of Hardware and Software and Basics of Technology for Electromagnetic Monitoring of Geodynamic Processes in Seismically Active Zones and Assessment of Their Hazard." Scientific topic code: FMNN-2019-0004. State registration no.: AAAA-A19-119020190065-6.

CONFLICT OF INTEREST

The authors declare that there is no conflict of interest.

REFERENCES

Aleksanova, E.D., Bobachev, A.A., Bol'shakov, D.K., Gorbunov, A.A., Ivanova, S.V., Kulikov, V.A., Modin, I.N., Pushkarev, P.Yu., Khmelevskoi, V.K., Shustov, N.L., and Yakovlev, A.G., *Elektrorazvedka: Posobie po elektrorazvedochnoi praktike dlya studentov geofizicheskikh spetsial'nostei* (Electrical Prospecting: A Guide to Electrical Exploration Practice for Students of Geophysical Specialties), Khmelevskoi, V.K., Modin, I.N., and Yakovlev, A.G., Eds., Moscow: GERS, 2005.

Bobrovskii, V.V., Software for Registering the Signals of the ERK ShPS Measuring Complex with Synchronous Accumulation in Real Time: Certificate of the Russian Federation on the State Registration of Computer Programs no. 2020613370, 2020.

Bobrovskii, V.V. and Il'ichov, P.V., Software for Processing the Data of Registration and Modeling of an Electrical Prospecting Complex with Noise-Like Signals: Certificate of the Russian Federation on the State Registration of Computer Programs no. 2018614566, 2018a.

Bobrovskii, V.V. and Il'ichev, P.V., Mathematical modeling of alleged sources (causes) of "structural interference" in geoelectrical prospecting equipment with pseudonoise sounding signals, *Problemy geodinamiki i geoekologii vnutrikontinental'nykh orogenov: Materialy dokl. VII Mezhdunar. simpoziuma, g. Bishkek, 19–24 iyunya 2017 g.* (Problems of Geodynamics and Geoecology of Inland Orogens: Proc. VII Int. Symposium), Rybin, A.K. and Zabinyakov, O.B., Eds., Bishkek: Nauchn. Stantsiya Ross. Akad. Nauk, 2018b, pp. 360–370.

Bobrovskii, V.V. and Il'ichov, P.V., Software for processing data of registration and modeling of an electrical prospecting complex with pseudonoise signals, *Vestn. Kyrg.-Ross. Slavyanskogo Univ.,* 2019, vol. 19, no. 12, pp. 77–83.

Duncan, P.M., Bailey, R.C., Edwards, R.N., Garland, G.D., and Ywang, A., The development and applications of a wide band electromagnetic sounding system using pseudo-noise source, *Geophysics,* 1980, vol. 45, no. 8, pp. 1276–1296.

Elektrorazvedka. Spravochnik geofizika (Electrical Prospecting. Geophysicist's Handbook), Khmelevskoi, V.K. and Bondarenko, V.M., Moscow: Nedra, 1989, book 1.

Groisman, F.E. and Trapeznikov, Yu.A., *Apparaturnye razrabotki dlya geofizicheskikh issledovanii elektromagnitnymi metodami* (Hardware Advances for Geophysical Research by Electromagnetic Methods), Moscow: Inst. Fiz. Zemli Akad. Nauk SSSR, 1986.

Il'ichev, P.V., Technological aspects of using pseudonoise signals in active geoelectrical prospecting systems, mathematical modeling, *Sovremennye problemy geodinamiki i geoekologii vnutrikontinental'nykh orogenov: Materialy 5-go Mezhdunarodnogo simpoziuma, g. Bishkek, 19–24 iyunya 2011 g.* (Current Problems of Geodynamics and Geoecology of Inland Orogens: Proc. 5th International Symposium, Bishkek, June 19–24, 2011), Leonov, M.G. and Sharov, N.V., Eds., Bishkek: Nauchn. Stantsiya Ross. Akad. Nauk, 2012, vol. 2, pp. 165–178.

Il'ichev, P.V. and Bobrovskii, V.V., Variations in the level of nonlinear distortions of electrical signals in the Earth's crust as a controlled parameter of geophysical monitoring, *Vestn. Kyrg.-Ross. Slavyanskogo Univ.,* 2018, vol. 18, no. 12, pp. 108–112.

Il'ichev, P.V. and Lashin, O.A., RU Patent 168302, 2017.

Il'ichov, P.V., Bragin, V.D., Shchelochkov, G.G., Bobrovskii, V.V., Myasnikov, D.S., and Zakupina, G.S., RU Patent 2408037, 2010.

Ilyichev, P.V. and Bobrovsky, V.V., Application of pseudonoise signals in systems of active geoelectric exploration (Results of mathematical simulation and field experiments), *Seism. Instrum.,* 2015, vol. 51, no. 2, pp. 53–64.

Lashin, O.A., Application of programmable logic integrated circuits in the development of geophysical measuring equipment, *Vestn. Kyrg.-Ross. Slavyanskogo Univ.,* 2018, vol. 18, no. 4, pp. 67–71.

Lashin, O.A., A probing signal generator for a modern electrical prospecting measuring complex, *Vestn. Kyrg.-Ross. Slavyanskogo Univ.,* 2019a, vol. 19, no. 12, pp. 83–87.

Lashin, O.A., A spectral analyzer for monitoring interference conditions in field geophysical research, *Sovremennye tekhnika i tekhnologii v nauchnykh issledovaniyakh: Sb. materialov XI Mezhdunar. konf. molodykh uchenykh i studentov* (Current Techniques and Technologies in Scientific Research: Proc. XI Int. Conf. of Young Researchers and Students), Zabinyakova, O.B., Ed., Bishkek: Nauchn. Stantsiya Ross. Akad. Nauk, 2019b, vol. 1, pp. 104–108.

Lisimov, M.O., Application of modern fiber-optic technology for the transmission of digital signals in geophysical measuring equipment, *Sovremennye tekhnika i tekhnologii v nauchnykh issledovaniyakh: Sb. materialov XI Mezhdunar. konf. molodykh uchenykh i studentov* (Current Techniques and Technologies in Scientific Research: Proc. XI Int. Conf. of Young Researchers and Students), Zabinyakova, O.B., Ed., Bishkek: Nauchn. Stantsiya Ross. Akad. Nauk, 2019, vol. 1, pp. 109–113.

Matveev, B.K., *Elektrorazvedka* (Electrical Prospecting), Moscow: Nedra, 1990.

Sidorov, V.A., *Impul'snaya induktivnaya elektrorazvedka* (Pulsed Inductive Electrical Prospecting), Moscow: Nedra, 1985.

Svetov, B.S., *Osnovy geoelektriki* (Fundamentals of Geoelectrics), Moscow: LKI, 2008.

Tietze, U. and Schenk, C., *Halbleiter-Schaltungstechnik,* Springer, 1999, 11th ed.

Trapeznikov, Yu.A. and Turovskii, P.S., RU Patent 1637549, 1993.

Trapeznikov, Yu.A., Bragin, V.D., Il'ichev, P.V., Orlenko, N.N., Ivanov, E.I., Matiks, A.I., and Konovalov, S.M., RU Patent 2091820, 1997.

Varakin, L.E., *Sistemy svyazi s shumopodobnymi signalami* (Communication Systems with Noise-Like Signals), Moscow: Radio i Svyaz', 1985.

Velikin, A.B., RU Patent 2354999, 2009.

Velikin, A.B. and Velikin, A.A., A new correlation method of pulsed electrical prospecting with pseudonoise signals STEM for electromagnetic sounding of subsoil in the search for hydrocarbon raw materials, *Vopr. Estestvozn.,* 2016, no. 1, pp. 100–103.

Volykhin, A.M., Bragin, V.D., Zubovich, A.V., Antonov, N.L., Babakov, Yu.P., Batalev, V.Yu., Blokh, A.G., Geller, E.L., Zeigarnik, V.A., Ivanov, E.I., Isaev, Yu.I., Koshkin, N.A., Kuz'min, R.K., Kulevtsova, T.I., Matiks, A.I., et al., *Proyavlenie geodinamicheskikh protsessov v geofizicheskikh polyakh* (Manifestation of Geodynamic Processes in Geophysical Fields), Moscow: Nauka, 1993.

Zhdanov, M.S., *Elektrorazvedka* (Electrical Prospecting), Moscow: Nedra, 1986.